https://doi.org/10.17221/73/2025-PSE

Halophytic resilience in extreme environments: adaptive strategies of *Suaeda schimperi* in the Red Sea's hyper-arid salt marshes

Farag Ibraheem[1]*, *Mohammed Albaqami*[2], *Eman M. Elghareeb*[3]*

[1]*Umm Al-Qura University, Al-Qunfodah University College, Biology and Chemistry Department, Al-Qunfodah, Saudi Arabia*
[2]*Botany and Microbiology Department, College of Science, King Saud University, Riyadh, Saudi Arabia*
[3]*Botany Department, Faculty of Science, Mansoura University, Mansoura, Egypt*
**Corresponding authors: emanmohammed@mans.edu.eg; fllbraheem@uqu.edu.sa*

Citation: Ibraheem F., Albaqami M., Elghareeb E.M. (2025): Halophytic resilience in extreme environments: adaptive strategies of *Suaeda schimperi* in the Red Sea's hyper-arid salt marshes. Plant Soil Environ., 71: 320–337.

Abstract: *Suaeda schimperi*, a halophyte native to the Red Sea's hyper-arid salt marshes, thrives in its extreme conditions (high salinity, minimal rainfall, and elevated temperatures). However, its adaptive tolerance mechanisms to these harsh conditions remain unclear. Herein, we investigated its growth responses and physiological mechanisms after short (5 days after treatment; DAT) and long-term (15 DAT) exposure to 0, 100, 200, and 400 mmol NaCl. Moderate salinity (200 mmol NaCl) enhanced growth, inducing 103.2% (5 DAT) and 40% (15 DAT) higher leaf biomass and 43.33% and 59.6% higher root biomass, respectively, compared to non-saline conditions. Deviation from moderate salinity reduced growth and disrupted ion balance, lowering K^+, raising Na^+, and increasing the Na^+/K^+ ratio, particularly under high salinity. The moderate salinity-enhanced growth was associated with increased chlorophyll, glycine betaine, glutathione, betacyanin, and betaxanthin, as well as higher antioxidant enzyme activity (polyphenol oxidase, peroxidase, catalase, ascorbate, and peroxidase) at 5 DAT. At 15 DAT, sugar accumulation and unsaturated fatty acids increased, while malondialdehyde and saturated fatty acids decreased. These findings reveal multiple adaptive strategies that support *S. schimperi's* physiological stability under extreme environments and highlight its significance in ecological restoration and breeding salt-tolerant crops under escalating soil salinisation and climate change.

Keywords: osmotic stress; saline habitat; adaptation; salt tolerance

Soil salinisation is a widespread agricultural challenge that limits plant growth and crop productivity worldwide (Pungin et al. 2023). Each year, it increases by 10%, driven by many factors including the use of poor-quality irrigation water, climate change, and anthropogenic activities that aggravate salt buildup in soils (Joshi et al. 2023, Ahmed et al. 2024). The deteriorative effects of salinity are attributed to its induced disruption of key physiological processes and metabolic pathways in plants *via* ionic toxicity, osmotic stress, and oxidative injury (Flowers and Colmer 2015). The salinity-induced buildup of Na^+ ions within plants disturbs ion homeostasis and plant osmotic potential, restricts the uptake and accumulation of water and nutrients, and impairs membrane stability, enzyme activity, and photosynthesis (Li et al. 2022). These salinity-elicited effects also initiate the production of reactive oxygen species (ROS), which trigger a cascade of oxidative damage to several cellular components, including DNA, proteins, and lipids (Panda et al. 2021). These disturbances lead to stunted growth, reduced biomass, and lower yields, particularly in salt-sensitive plants (Guo et al. 2020).

This research work was funded by Umm Al-Qura University, Saudi Arabia under grant number: 25UQU4350597GSSR01.

https://doi.org/10.17221/73/2025-PSE

Interestingly, halophytes which make up less than 2% of the world's flora, thrive in extremely saline habitats (Hussain and Khan 2022). Unlike glycophytes that suffer damage at 50 mmol NaCl, halophytes can grow, reproduce, and complete their life cycle at 400 mmol or even more (Ibraheem et al. 2022). To cope with such high salinity levels, halophytes have evolved various physiological, metabolic, and molecular adaptive strategies that synergistically protect them from the harsh saline environment (Pungin et al. 2023). For instance, halophytes efficiently manage the flux, accumulation, exclusion, and compartmentalisation of Na^+ and K^+ ions at both cellular and whole-plant levels to combat salt-stress damage (Joshi et al. 2023). Another key salt tolerance strategy in halophytes involves accumulating compatible solutes like sugars, proline, and glycine betaine (GB), which contribute to osmotic adjustment and stabilisation of cell membranes and proteins under salt stress (Kumar et al. 2021). Additionally, halophytes employ complex enzymic- and non-enzymic antioxidant defence mechanisms to protect plant cells against salinity-induced oxidative stress. Key antioxidant enzymes include catalase (CAT), peroxidase (POX), superoxide dismutase (SOD), ascorbate peroxidase (APX), and glutathione reductase (GR) (Pirasteh-Anosheh et al. 2023). The non-enzymatic antioxidant defence system includes secondary metabolites like glutathione (GSH), betacyanin, betaxanthin, ascorbate (AsA), carotenoids, flavonoids, and phenolics, all of which play a crucial role in maintaining the delicate balance between ROS production and scavenging, thereby regulating the cellular redox state under elevated salinity (Castillo et al. 2022, Cai et al. 2025). The efficiency of the plant antioxidant system is a central determinant of the remarkable ability of halophytes to survive under saline conditions (Pirasteh-Anosheh et al. 2023). Moreover, the modulation of fatty acid composition in biological membranes contributes to the halophytes' adaptive mechanisms *via* regulating membrane fluidity under severe salinity stress (Behr et al. 2017, Zang et al. 2021). Despite the importance of membrane lipids in salinity tolerance, the alterations in the composition of membrane fatty acids in halophytes received relatively little attention. Furthermore, the mechanisms behind stress tolerance in many halophytic species remain largely unclear. Therefore, further research into salinity tolerance, stress signalling, and detoxification pathways in more halophytic species is necessary to enhance our understanding of salt tolerance and to advance knowledge for improving crop resilience in salt-affected lands. Halophytes provide unique and valuable resources for candidate genes/factors for developing sustainable agriculture in saline-affected soils (Mujeeb et al. 2021).

The *Suaeda* genus belongs to Amaranthaceae (formerly known as Chenopodiaceae) and is naturally adapted to high salinity levels in salt marshes. *Suaeda* species provide a unique model system for the dissection of salt resilience in halophytes at both physiological and molecular levels (Diao et al. 2021, Ibraheem et al. 2022). Most studies have focused on more common *Suaeda* species, while little is known about the stress physiology of rare and geographically restricted species such as *S. schimperi* (Moq.) Ulbr. The presence of *S. schimperi* has been reported in Saudi Arabia (Collenette 1985), Somalia (Thulin et al. 2008), Egypt (Boulus 1999), Sudan (Darbyshire et al. 2015), Ethiopia, and Eritrea (Edwards et al. 2000). Unlike other *Suaeda* species, *S. schimperi* is native to extremely harsh and saline environments along the Red Sea coast, which may have driven the evolution of distinct physiological adaptations. This makes it a valuable, yet underexplored, candidate for studying salt tolerance mechanisms in extreme conditions. Recently, we explored *S. schimperi* plants' adaptation to salinity, elemental disorder, and toxic elements in their natural salt marshes on the east coast of the Red Sea. We also reported their capacity in the biosynthesis of betacyanin as an efficient antioxidant and their potential as phytoextractors of toxic elements from their environment (Ibraheem et al. 2022). However, the species' growth and physiological responses under controlled salt stress conditions remain unclear. Specifically, its optimal growth range under salinity, its mechanisms for adjusting osmotic potential and maintaining water availability, photosynthesis and carbon assimilation, and the role of stress-related osmolytes such as proline and glycine betaine, if any, are not fully understood. Therefore, the current study aims to (1) assess the growth responses of *S. schimperi* under increasing salinity stress and (2) investigate the mechanisms of osmotic adjustment and oxidative stress defence and how they relate to photosynthesis, carbon assimilation, and overall salt resilience. Thus, pot-grown *S. schimperi* plants were exposed to different salinity levels, and samples were harvested at different time points post-salt application to evaluate their growth and physiological responses.

https://doi.org/10.17221/73/2025-PSE

MATERIAL AND METHODS

Plant material, growth conditions, and maintenance. Seeds of *Suaeda schimperi* (Moq.) Ulbr. were collected from a single plant growing in the salt marsh on the east coast of the Red Sea (longitude: 41.0644571, latitude:19.1494134) at Al-Qunfodah governorate, Saudi Arabia. The seeds were cleaned and kept at 4 °C. Uniform seeds were sown in germination trays filled with clean acid-washed sand and irrigated with a quarter-strength nutrient solution, prepared according to the full-strength composition described previously (Behr et al. 2017). Plants were maintained under natural day/night cycle conditions, temperature, and humidity for 28 days. Subsequently, plantlets with uniform morphological features were transplanted into 60 plastic pots (30 cm wide, 40 cm deep) filled with clean acid-washed sand. The transplanted plants were initially irrigated with the same nutrient solution twice a week, with a stepwise increase in the concentration of the nutrient solution until it reached full strength. Plant growth was supported by a full-strength nutrient solution for another four weeks. Subsequently, pots with uniform plant growth were allocated into four groups (three biological replicates, 8 pots each, 3 plants/pot) and used for the application of different levels of salinity stress. During the experimental period, the average daytime temperature was 28 °C, with maximum temperature reaching up to 32 °C and minimum temperature around 24 °C; nighttime temperature dropped to approximately 17 °C. The average relative humidity was approximately 54%. The region also received an average of 9 h of sunshine per day, with about 11 daylight hours.

Salinity stress application, plant growth, and tissue harvest. Four levels of salt stress (0, 100, 200, and 400 mmol NaCl) were applied by gradually introducing NaCl increments of 0, 25, 50, and 100 mmol, respectively, with each successive irrigation to avoid osmotic shock. This process ensured that the final salinity levels were reached simultaneously, two weeks after the initial salt treatment (Hameed et al. 2012). The moisture content of the pots was kept at field capacity using tap water. Plants were harvested 5 and 15 days after completion of salt treatment (DAT). Six plants/treatments were harvested at each time point, divided into two subsets (three plants each), and processed based on downstream analyses. The first subset was used to assess growth parameters and biomass allocation, as well as analysis of various carbohydrate fractions, elemental composition, non-enzymic antioxidants, and fatty acids profiling. Leaves from the second subset were snap-frozen in liquid nitrogen, ground into a fine homogenous powder, stored at –80 °C, and used to analyse photosynthetic pigments, oxidative stress markers, and antioxidant enzyme activity.

Morphological traits and growth analysis. Plants from the first subset were separated into leaves, stems, and roots, and their fresh weights (FWT) were recorded using an analytical balance. The samples were then dried to constant weights in an electric oven at 65 °C, and the dry weights (DWT) were recorded.

Photosynthetic pigments analysis. Chlorophyll *a* (Chl *a*) and chlorophyll *b* (Chl *b*) were quantified as described previously (Lichtenthaler and Wellburn 1983). Frozen powdered leaf tissues (50 mg) were extracted in chilled 80% acetone. The absorbance of the clear extracts was measured at 646 and 663 nm for chlorophyll *a* and *b*, respectively, using a spectrophotometer (PD-303UV, APEL, Saitama, Japan). Chlorophyll concentrations were determined using the following equations and expressed as mg/g FWT:

$$\text{Chl } a = (12.25\ A663 - 2.79\ A646)$$

$$\text{Chl } b = (21.21\ A646 - 5.1\ A663)$$

Betalain pigments analysis. Aliquots of the frozen leaves (500 mg) were homogenised in 10 mL cold methanol for 30 min and centrifuged at 4 °C for 10 min at 10 000 rpm. The supernatants were removed, and the pellets were extracted at 4 °C in distilled water. The levels of betacyanin and betaxanthin were determined spectrophotometrically (PD-303UV, APEL, Saitama, Japan) at 538 and 470 nm, respectively, and quantified by using the molar extinction coefficient 60 000 for betacyanin and 48 000/mol/cm for betaxanthins (Skalicky et al. 2020).

Carbohydrate fraction analysis. Aliquots of dried and powdered leaf samples (100 mg) were extracted in 80% aqueous ethanol. The alcoholic extracts were utilised for spectrophotometric (PD-303UV, APEL, Saitama, Japan) quantification of total soluble sugars (TSS) and sucrose using the anthrone-sulfuric acid method at 620 nm (Hansen and Møller 1975). The insoluble fractions of the leaf tissues were used for the determination of starch by hydrolysis in a mixture of perchloric acid and water in a 6.5:1 ratio. The obtained sugars from starch hydrolysis were quantified using the anthrone method (Sadasivam 1996). Carbohydrate content was determined based on a standard glucose curve and expressed as mg/g DWT.

Quantification of elements. Dried and powdered leaf tissues (100 mg) were digested in nitric acid and

https://doi.org/10.17221/73/2025-PSE

used for the determination of the sodium (Na^+) and potassium (K^+). Na^+ and K^+ levels were measured using the flame photometric method (MODEL 360, Sherwood Scientific, Cambridge, UK).

Oxidative stress marker assessment. Malondialdehyde (MDA) as an indicator of lipid peroxidation was assessed using the thiobarbituric acid (TBA) method, as reported by Ouyang et al. (2010). Frozen leaf tissues (500 mg) were macerated in 5 mL 10% (*w*/*v*) TBA. The homogenate was centrifuged at 4 000 rpm for 10 min at 4 °C. Afterwards, 0.5 mL of the supernatant was added to 0.5 mL of 0.6% (*w*/*v*) TBA. The mixture was heated for 30 min in a water bath at 95 °C, then quickly cooled in an ice bath before being spun at 12 000 rpm for 10 min. The absorbance of the supernatant was recorded at 532 and 600 nm (PD-303UV, APEL, Saitama, Japan), and the MDA concentration was determined using an extinction coefficient of 155 and finally expressed as nmol/g FWT. Endogenous H_2O_2 content was assessed following the method of Alexieva et al. (2001). Aliquots of 0.5 mL of leaf extracts were combined with 0.5 mL of phosphate buffer (100 mmol, pH 7.0) and 2 mL of 1 mol KI solution. The mixtures were kept in the dark for 1 h before recording the absorbance at 390 nm. H_2O_2 level was determined using a spectrophotometer (PD-303UV, APEL, Saitama, Japan) and a standard curve, then expressed as µmol/g FWT.

Proline and glycine betaine measurement. Proline content was determined using the sulfosalicylic acid (SSA) method. Aliquots (0.5 g) of the dried and powdered leaves were extracted in 3% sulfosalicylic acid and filtered (Bates et al. 1973). Next, 2 mL of the extracts were mixed with acidic ninhydrin and heated for 25 min in a boiling water bath. The reaction mixtures were thoroughly agitated with 4 mL of toluene. The absorbance of the developed colour was recorded at 520 nm by a spectrophotometer (PD-303UV, APEL, Saitama, Japan) and the proline concentration was calculated from a standard curve and expressed in µg/g FWT. Glycine betaine content was measured as described previously (Grieve and Grattan 1983). Aliquots (0.1 g) of leaf tissues were macerated in 15 mL of deionised water and filtered. The clear filtrates were diluted 1:1 using 2 mol H_2SO_4, cooled on ice for 1 h, and centrifuged for 15 min at 4 °C at 13 000 rpm. One mL of the clear supernatants was combined with 0.5 mL of cold potassium triiodide solution (7.5 g iodine mixed with 10 g potassium iodide and dissolved in 1 mol HCl). The mixtures were gently stirred, maintained at 4 °C for 16 h, and centrifuged at 12 000 rpm for 15 min. The formed periodide crystals were dissolved in 9 mL of 1,2-dichloroethane, and the mixtures were left to set for 2 h, and the absorbance was determined at 365 nm (PD-303UV, APEL, Saitama Japan). GB concentration was determined from a standard curve and expressed as mg/g DWT.

Glutathione estimation. Aliquots of frozen leaf tissues (500 mg) were macerated in 5 mL of cold extraction buffer (50 mmol potassium phosphate, pH 7.5, 1 mmol EDTA). The extracts were spun at 4 000 rpm and 4 °C for 15 min. The resulting supernatants were processed for spectrophotometric determination (PD-303UV, APEL, Saitama, Japan) of glutathione (GSH) by the Biodiagnostic kit (GR 2511). The method is based on the ability of GSH to reduce 5,5'-dithiobis (2-nitrobenzoic acid) (DTNB) to a chromogen whose absorbance at 405 nm is proportional to GSH concentration. Briefly, 0.5 mL of extract was combined with 0.5 mL of 500 mmol TCA and centrifuged for 15 min at 3 000 rpm. Then, 0.5 mL of the supernatant was mixed with 0.1 mL of DTNB reagent and 0.5 mL of buffer. After 10 min, the optical density was measured at 405 nm against a blank. GSH content was calculated and expressed as mmol/g FWT.

Antioxidant enzyme activity determination. CAT, POX, APX, and PPO were extracted by macerating 0.1 g of frozen leaf tissues in extraction phosphate buffer (0.02 mol, pH 7) at 4 °C. After spinning at 12 000 rpm at 4 °C for 20 min, the supernatants were used to assess the activity of antioxidant enzymes activity (Agarwal and Shaheen 2007). The activity of CAT was determined, as reported previously (Sinha 1972). Aliquots of enzyme extracts (0.5 mL) were incubated with 1 mL phosphate buffer (0.2 mol, pH 7.0, 0.4 mL of distilled water, and 0.5 mL of H_2O_2) for 1 min at 25 °C. The enzymatic reactions were stopped by the addition of 2 mL of an acid reagent (dichromate/acetic acid mixture), and the mixtures were heated for 10 min. The optical density was measured at 610 nm (PD-303UV, APEL, Saitama, Japan), and H_2O_2 concentration was calculated and expressed as mmol H_2O_2/min/g FWT. APX activity was assessed by monitoring the oxidation of ascorbate, indicated by a decline in the absorbance at 290 nm. The reaction mixtures were initiated by adding aliquots (0.050 mL) of the enzyme extracts to a mixture of 0.5 mL phosphate buffer (0.02 mol, pH 7), 0.075 mL H_2O_2 (2 mmol), and 100 µL ascorbate (0.5 mmol). APX activity was determined using an extinction coefficient

https://doi.org/10.17221/73/2025-PSE

of 2.8 mmol/cm and expressed as mmol of ascorbate/min/g FWT. POD activity was assayed, as reported by Devi (2002). The reaction buffer included 3 mL phosphate buffer (0.1 mol, pH 6) containing pyrogallol (0.05 mol) and 0.5 mL H_2O_2 (1%). The reactions were initiated by adding 0.1 mL of enzyme extract, followed by incubation at room temperature for 1 min. The activity of POD was calculated and expressed as U/min/g FWT. The PPO activity was monitored following the method described by Raymond et al. (1993). Briefly, the reaction mixtures contained 1 mL enzyme extract, 2 mL phosphate buffer (0.02 mol, pH 7), and 1 mL of pyrogallol (0.1 mol) in a 4 mL final volume. Enzyme activity was measured at 430 nm and expressed as U/min/g FWT.

Determination of fatty acids composition. Aliquots (1 g) of powdered dry leaf tissue were extracted in n-hexane for 24 h using a Soxhlet apparatus. The fatty acid composition of the extracted lipids was examined using gas chromatography (GC-FID), as described previously (Zahran and Tawfeuk 2019). Quantities (15 mg) of lipids were mixed with 1 mL of n-hexane, vortexed for 30 s, combined with 1 mL of sodium methoxide (0.4 mol), and revortexed for another 30 s. The mixtures were allowed to settle at room temperature for 15 min. The upper phase, containing the fatty acid methyl esters (FAMEs), was collected and analysed using GC-FID. The FAMEs were analysed using an HP 6890 plus gas chromatography (Hewlett Packard, Wilmington, USA) equipped with a Supelco™ SP-2380 capillary column (30 m × 0.25 mm × 0.20 µm) (Sigma-Aldrich, USA). The flame ionisation detector (FID) and the injector were maintained at 260 °C. The column temperature was initially set at 50 °C for 3 min, then increased to 225 °C (17.5 min) at a rate of 10 °C/min and held at 225 °C (10 min). Helium served as the carrier gas at a 1.2 mL/min flow rate. FAMEs were detected by matching their relative and absolute retention times with those of authentic FAMEs standards (from C4:0 to C24:0). The quantification was performed using the manufacturer's integrated data-processing software (Santa Clara, USA). The fatty acid composition was expressed as a relative percentage of the total peak area.

Statistical analysis. The experiment was conducted using a completely randomised block design. Duncan's multiple range test was employed to decide the statistically significant difference ($P < 0.05$) among means ($n = 3$) of different responses for various salt stress treatments. The data were analysed using one-way analysis of variance (ANOVA) using XL-STAT software (Addinsoft, Paris, France) and presented as the mean ± standard error (SE). Metaboanalyst 6.0 (https://www.metaboanalyst.ca) was used to construct principal component analysis (PCA), heatmap, and correlation matrix.

RESULTS

Growth of *S. schimperi* under salinity stress. Figure 1 shows the impact of varying salt stress levels on the growth of *S. schimperi* at 5 DAT and 15 DAT. At both time points, leaf fresh weight and biomass peaked at 200 mmol NaCl, while lower and higher salinity levels significantly reduced these growth parameters. Compared to non-saline conditions, plants grown under 200 mmol salinity level had 69.76% higher leaf fresh weight and 103.29% more leaf biomass at 5 DAT. The corresponding values of these two parameters were 87.89 and 40% at 15 DAT. Root fresh weight and biomass followed similar patterns with a notable improvement in these parameters under low salinity level (100 mmol), particularly at 15 DAT. Compared to the non-salinised plants, the 200 mmol-treated plants had 32.6% higher root fresh weight and 43.33% more root biomass at 5 DAT and 27.5% and 59.6% at 15 DAT.

Ionic content in *S schimperi* under salinity stress. Increasing salinity levels significantly increased the cellular Na^+ concentration in leaves with the highest induction (up to 3.3-fold) under high salt stress (400 mmol NaCl) at 15 days, compared to non-saline conditions (Figure 2). Conversely, the K^+ concentration significantly decreased with increasing salt concentration. At both the 5 and 15 DAT, 400 mmol NaCl resulted in the highest reduction in K^+ content, with ~ 38.43% and 60% lower than the non-salinised plants, respectively. Such alterations in cellular Na^+ and K^+ responses were reflected in significant variation in Na^+/K^+ ratio, which significantly increased in all salinity-treated plants, most notably in 400 mmol NaCl-treated plants at 15 days, which had 8.4-fold higher Na^+/K^+ than their non-salt stressed peers.

Changes in chlorophyll content in *S. schimperi* under salinity stress. The levels of Chl *a* and Chl *b* exhibited varying responses to salt treatments at 5 and 15 DAT (Figure 3). Compared to the non-saline conditions, the medium salt concentration triggered a 42.86% increase in Chl *a*, however, this effect was less pronounced at 15 DAT. In contrast, low and high salt concentrations elicited a slight decrease in Chl *a* at both sampling times. Regarding Chl *b*, all salt treatments initially increased Chl *b* content

https://doi.org/10.17221/73/2025-PSE

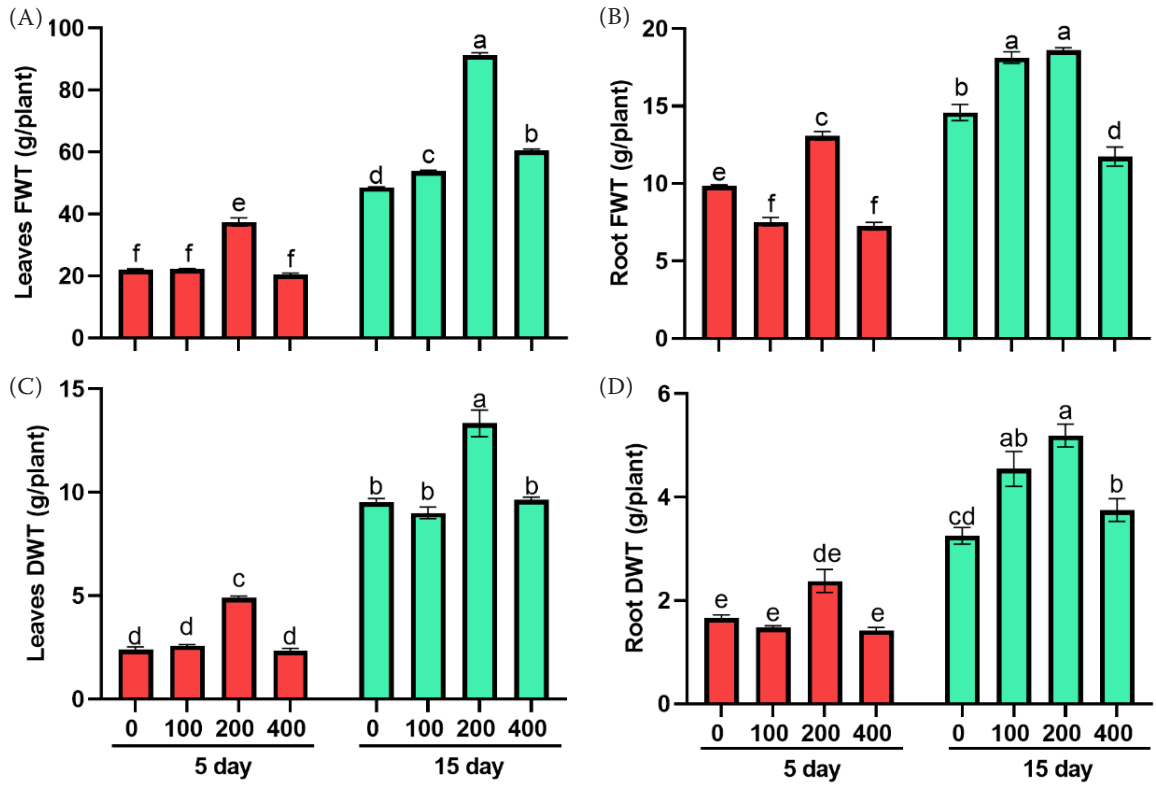

Figure 1. Changes in growth-related parameters of *Suaeda schimperi* plants grown under 0, 100, 200, and 400 mmol NaCl after 5 and 15 days of salt application. Shown are (A) leaves fresh weights (FWT); (B) root FWT; (C) leaves dry weights (DWT). and (D) root DWT. Bars denote means ± standard error (n = 3). Different letters designate significant differences among means at $P < 0.05$, whereas similar letters indicate non-significant differences according to Duncan's test

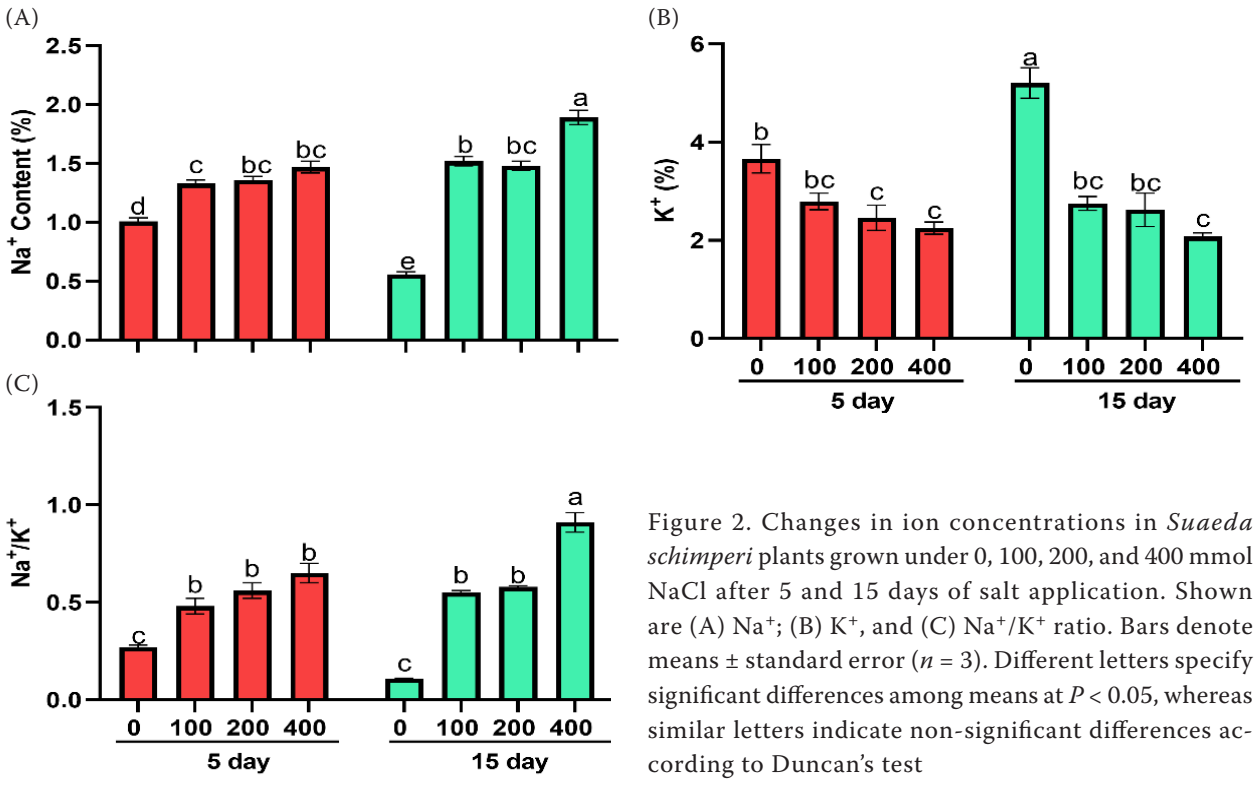

Figure 2. Changes in ion concentrations in *Suaeda schimperi* plants grown under 0, 100, 200, and 400 mmol NaCl after 5 and 15 days of salt application. Shown are (A) Na^+; (B) K^+, and (C) Na^+/K^+ ratio. Bars denote means ± standard error (n = 3). Different letters specify significant differences among means at $P < 0.05$, whereas similar letters indicate non-significant differences according to Duncan's test

https://doi.org/10.17221/73/2025-PSE

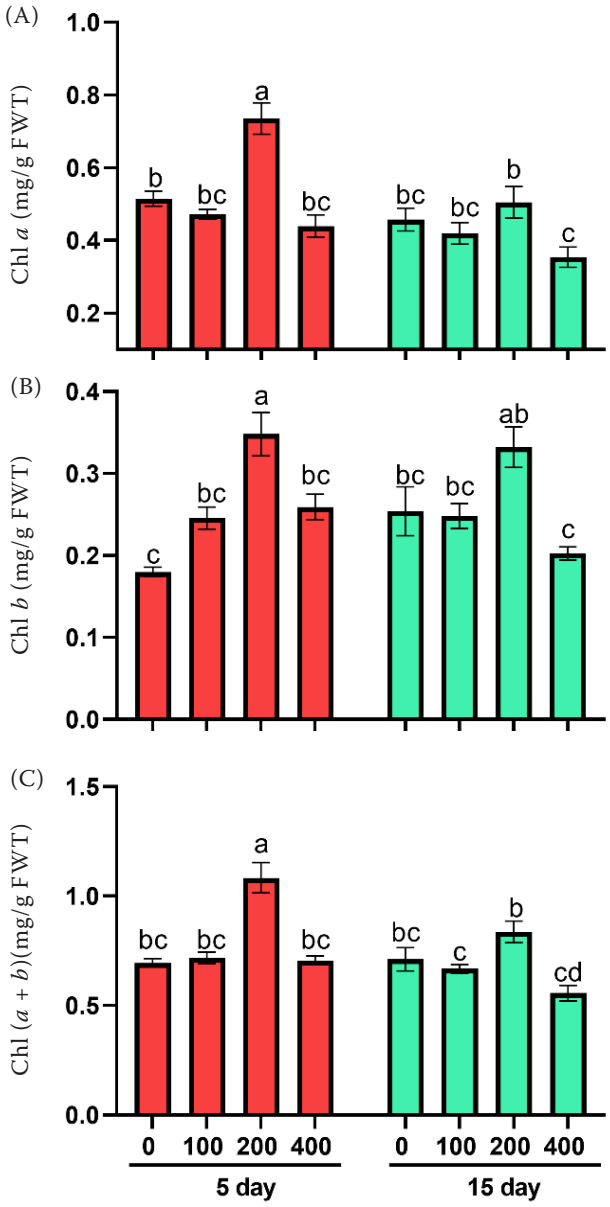

Figure 3. Changes in chlorophyll pigments in *Suaeda schimperi* plants grown under 0, 100, 200, and 400 mmol NaCl after 5 and 15 days of salt application. Shown are (A) chlorophyll *a* (chl *a*); (B) chlorophyll *b* (chl *b*), and (C) chlorophyll (*a* + *b*). Bars denote mean ± standard error (*n* = 3). Different letters designate significant differences among means at $P < 0.05$, whereas similar letters specify non-significant differences according to Duncan's test. FWT – fresh weights

at 5 DAT, and the highest induction (102.62%) was observed under 200 mmol treatment compared to the non-saline conditions. At 15 DAT, the Chl *b* level was either marginally increased (200 mmol) or non-significantly changed (100 and 400 mmol). Total chlorophyll responses mirrored that of Chl *a* at both time points.

Changes in carbohydrate fractions in *S. schimperi* under salinity stress. Different salinity stress levels induced distinct responses in various carbohydrate fractions at both time points (Figure 4). At 5 DAT,

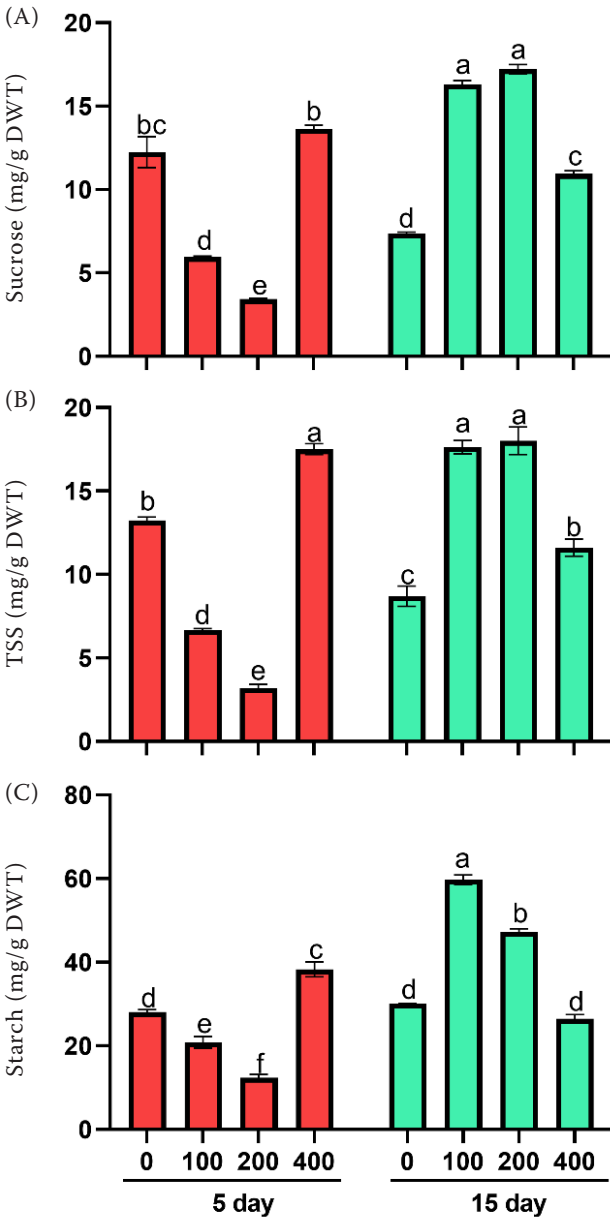

Figure 4. Changes in carbohydrate fractions in *Suaeda schimperi* plants grown under 0, 100, 200, and 400 mmol NaCl after 5 and 15 days of salt application. Shown are (A) sucrose; (B) total soluble sugars (TSS), and (C) starch. Bars denote means ± standard error (*n* = 3). Different letters designate significant differences among means at $P < 0.05$, whereas similar letters specify non-significant differences according to Duncan's test. DWT – dry weights

https://doi.org/10.17221/73/2025-PSE

low and moderate salt stress (100 and 200 mmol NaCl) decreased the content of TSS, sucrose, and starch compared to the non-saline conditions. The 200 mmol-treated plants had the lowest levels of sugars. In contrast, high salt stress (400 mmol NaCl) significantly increased the levels of these sugars relative to the non-saline conditions. At 15 DAT, all salinity levels enhanced the accumulation of TSS and sucrose compared to the non-stressed conditions. Interestingly, the highest salinity-induced increases in TSS (133.32%) and sucrose (107.15%) were noted in plants grown under 200 mmol NaCl. The greatest salinity-elicited increase for starch was observed in response to 100 mmol NaCl treatment at 15 DAT.

Changes in oxidative stress markers in *S. schimperi* under salinity stress. The salinity-induced responses in MDA and H_2O_2 levels, as key markers for oxidative stress, are shown in Figure 5. At 5 DAT, only the low salinity treatment significantly increased MDA accumulation by 21% compared to the non-saline conditions. At 15 DAT, *S. schimperi* plants subjected to moderate salt stress exhibited the lowest MDA levels across treatments, showing a 29% reduction relative to the non-stressed plants. In contrast, those under high salinity stress had the highest MDA level, 13.1% greater than the non-saline conditions. Regarding H_2O_2, all salinity treatments led to comparable but significantly elevated H_2O_2 levels relative to the non-stressed plants at 5 DAT. By 15 DAT, H_2O_2 levels had markedly increased compared to 5 DAT, with low and medium-salt-stressed plants showing significantly higher H_2O_2 accumulation than their non-stressed and highly stressed counterparts.

Changes in stress-associated osmotica in *S. schimperi* under salinity stress. Compared to the

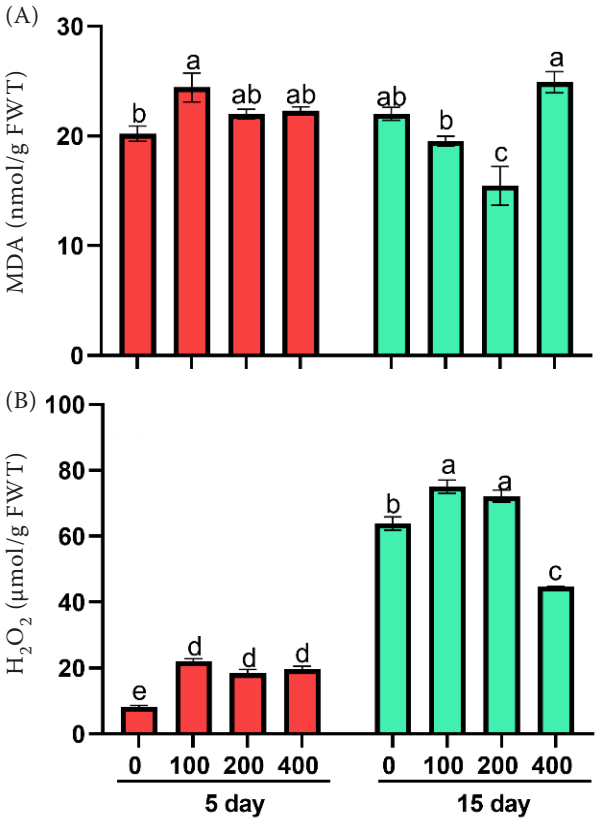

Figure 5. Changes in oxidative stress markers in *Suaeda schimperi* plants grown under 0, 100, 200, and 400 mmol NaCl after 5 and 15 days of salt application. Shown are (A) malondialdehyde (MDA) and (B) hydrogen peroxide (H_2O_2). Bars denote means ± standard error (n = 3). Different letters designate significant differences among means at $P < 0.05$, whereas similar letters specify non-significant differences according to Duncan's test. FWT – fresh weights

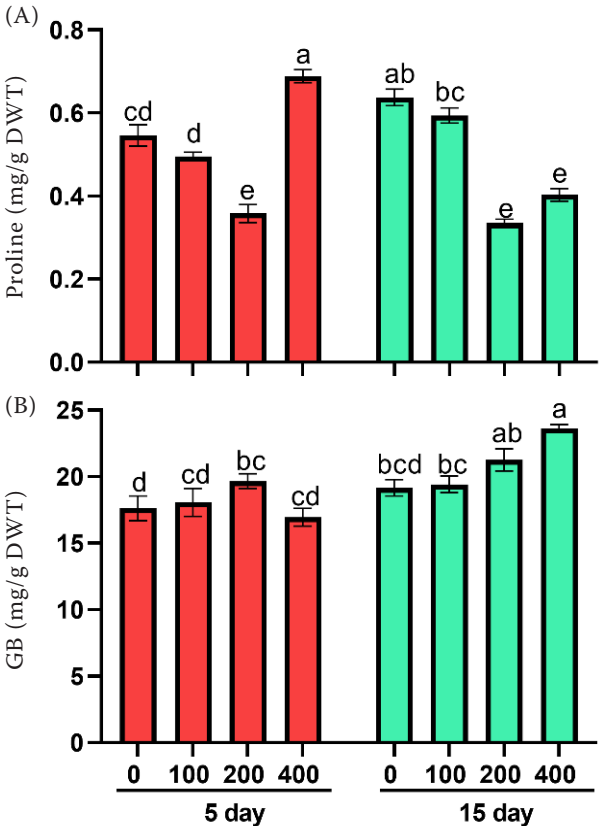

Figure 6. Changes in osmolytes in *Suaeda schimperi* plants grown under 0, 100, 200, and 400 mmol NaCl after 5 and 15 days of salt application. Shown are (A) proline and (B) glycine betaine (GB). Bars denote means ± standard error (n = 3). Different letters designate significant differences among means at $P < 0.05$, whereas similar letters specify non-significant differences according to Duncan's test. DWT – dry weights

https://doi.org/10.17221/73/2025-PSE

non-saline conditions, both lower and moderate salinity levels decreased proline content at 5 and 15 DAT, with the reduction being more pronounced under moderate salinity at both time points (Figure 6A). In contrast, the high salinity level induced the highest proline accumulation across all treatments at 5 DAT. However, by 15 DAT, proline levels significantly declined under high salinity, reaching a level like that observed at 200 mmol. Regarding GB, only plants under 200 mmol salinity exhibited significantly higher GB content than non-saline conditions. Other salinity levels resulted in GB accumulation similar to that of non-stressed conditions at 5 DAT (Figure 6B). By 15 DAT, GB levels were significantly ($P < 0.05$) elevated under both 200 mmol and 400 mmol salt treatments, with more pronounced increase (23%) under high salinity than moderate salinity (11%) relative to non-saline conditions.

Changes in non-enzymic antioxidants in *S. schimperi* under salinity stress. Active changes in the concentrations of a set of secondary metabolites, including GSH, betacyanin, and betaxanthin, were detected under varying salinity levels at both 5 and 15 DAT (Figure 7). Low and moderate salinity levels significantly increased GSH content at both 5 and 15 DAT compared to the non-saline conditions. High salinity level only boosted GSH at 15 DAT while having minimal effects at 5 DAT. Across treatments and time points, the 200 mmol-treated plants tended to have the highest average GSH levels. Also, the GSH levels were generally higher at 15 DAT than at 5 DAT. Interestingly, betacyanin followed a similar pattern with more distinctive differences among treatments. The moderate salinity caused 76.60% and 85.20% higher betacyanin than those under non-saline conditions at 5 and 15 DAT, respectively. High salinity level induced betacyanin accumulation at 15 DAT while its effect was marginal at 5 DAT. Similarly, betaxanthin increased as the salinity stress increased, peaking at 200 mmol NaCl and then declining at 400 mmolat 5 and 15 DAT.

Changes in antioxidant enzymes in *S. schimperi* under salinity stress. Different salinity stress levels stimulated active alterations in the activity of oxidative stress-related enzymes, including PPO, POD, CAT, and APX. At 5 DAT, the activities of these antioxidant enzymes increased as salinity rose, peaking at 200 mmol NaCl and then declining at 400 mmol, albeit at significantly different magnitudes (Figure 8). For instance, the 200 mmol NaCl treatment induced 5.0-, 3.7-, 3.96-, and 5.8-fold increase in the activities of PPO, POD, CAT, and APX, respectively, compared to the non-stressed conditions. Both low (100 mmol) and high (400 mmol) salinity stresses also induced the activities of these enzymes, though to slightly higher levels than the non-saline conditions. Relatively little variations in the activities of these enzymes were noted at 15 DAT. For example, plants grown under high salinity stress (400 mmol)

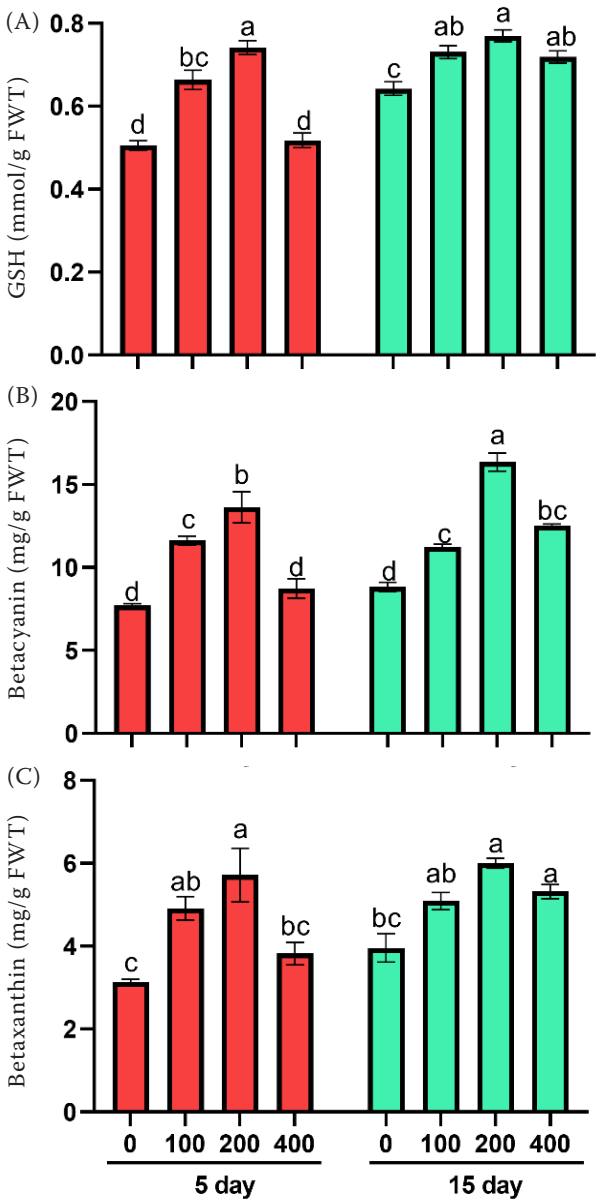

Figure 7. Changes in non-antioxidants in *Suaeda schimperi* plants grown under 0, 100, 200, or 400 mmol NaCl after 5 and 15 days of salt application. Shown are (A) glutathione (GSH); (B) betacyanin, and (C) betaxanthin. Bars denote means ± standard error ($n = 3$). Different letters designate significant differences among means at $P < 0.05$, whereas similar letters specify non-significant differences according to Duncan's test. FWT – fresh weights

https://doi.org/10.17221/73/2025-PSE

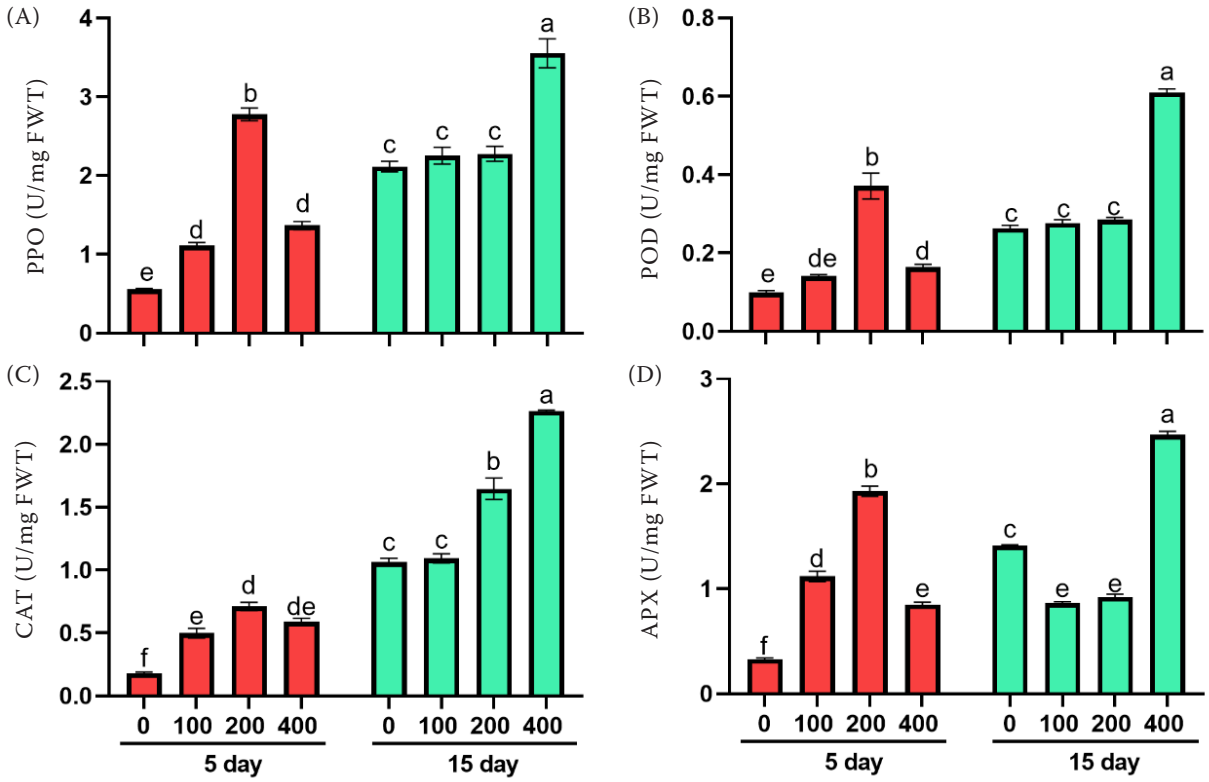

Figure 8. Changes in antioxidant enzymes in *Suaeda schimperi* plants grown under 0, 100, 200, and 400 mmol NaCl after 5 and 15 days of salt application. Shown are (A) polyphenol oxidase (PPO); (B) peroxidase (POD); (C) catalase (CAT), and (D) ascorbate peroxidase (APX). Bars denote means ± standard error (n = 3). Different letters designate significant differences among means at $P < 0.05$, whereas similar letters specify non-significant differences according to Duncan's test. FWT – fresh weights

had the highest PPO, POD, CAT, and APX activities among treatments. Also, plants grown under low and medium salinity stress had similar (PPO and POD) or lower (APX) activities than those under non-saline conditions. Furthermore, plants under low salt concentration had CAT activities like the non-stressed plants, whereas those under medium salt level had significantly higher CAT activity than their counterparts under non-saline conditions.

Changes in fatty acid composition in *S. schimperi* under salinity stress. Figure 9 presents a snapshot of the effects of varying salinity stress levels on the composition of the fatty acid pool in leaves of *S. schimperi* at 15 DAT. Under non-stressed conditions, *S. schimperi* leaves had a relatively high content of both palmitic (16:0) and stearic (C18:0) acids but significantly lower levels of palmitoleic (C16:1) and linoleic (C16:1) acids. Under salinity stress, the low salinity level induced the highest level of palmitic and stearic. The levels of these two acids dropped as salinity increased with the lowest levels observed at 200 mmol and with a slight recovery at 400 mmol NaCl. Compared to the non-stressed conditions, the moderate salinity-induced reductions in these two fatty acids approached 45.2% and 50.14% while those induced by high salinity levels were 37% and 27.4%. For palmitoleic and linoleic, their levels increased as salinity increased, peaking at 200 mmol and declining at 400 mmol NaCl, however, levels remained higher than low salinity level and non-stressed conditions.

Multivariate analysis. PCA analysis was carried out to visualise the variation in the tested parameters between non-salinised and salinised stress conditions. The score plot of the first two PCs in Figure 10A showed a discrete separation between four groups of 0, 100, 200, and 400 mmol NaCl treatments, explaining about 80.75% of the total variation, out of which 51.02% and 29.73% are represented in PC1 and PC2, respectively (Figure 10B). The PCA biplot in Figure 10C illustrates the multivariate relationships between physiological and biochemical features under different salinity levels (0, 100, 200, and 400 mmol). The traits such as fresh and dry weights (RFWT, LFWT, LDWT, RDWT), chlorophylls (Chl *a*, Chl *b*, TCH),

https://doi.org/10.17221/73/2025-PSE

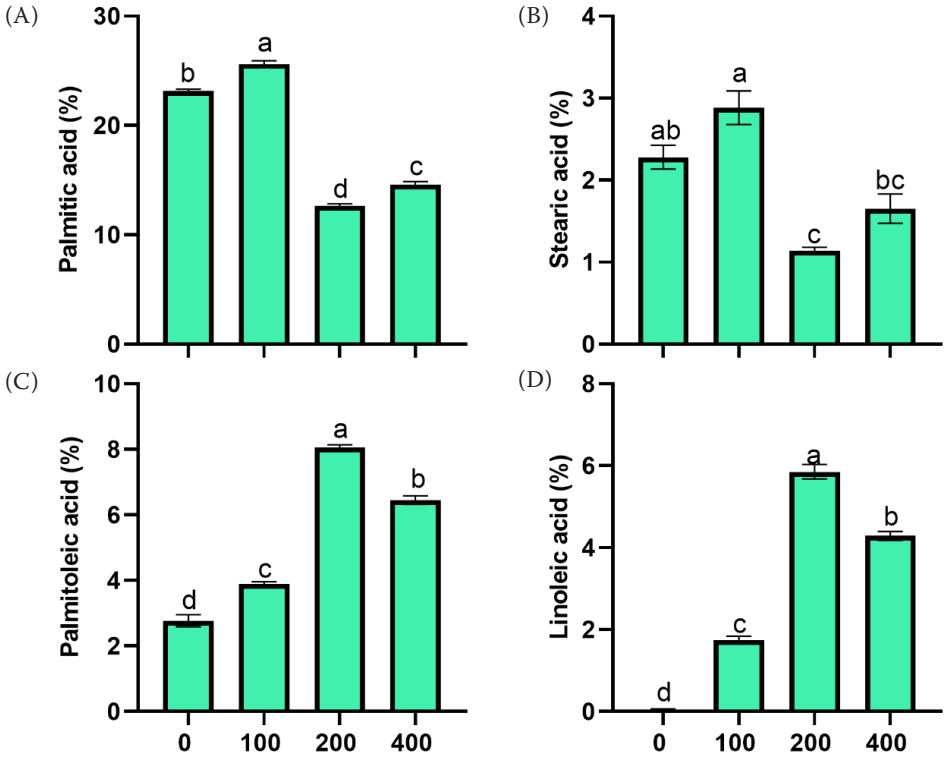

Figure 9. Changes in fatty acids composition in *Suaeda schimperi* leaves grown under 0, 100, 200, and 400 mmol NaCl after 15 days of salt application. Shown are (A) palmitic acid; (B) stearic acid; (C) palmitoleic acid, and (D) linoleic acid. Bars denote means ± standard error (n = 3). Different letters designate significant differences among means at $P < 0.05$, whereas similar letters specify non-significant differences according to Duncan's test

GB, GSH, betalains, PPO, palmitoleic, and linoleic acids are positively associated with moderate salinity level (200 mmol). Moreover, Na^+, Na^+/K^+, MDA, sucrose, TSS, starch, and CAT are highly expressed under 400 mmol NaCl treatment. POD and APX antioxidant enzymes contribute to both PC1 and PC2. The correlation matrix between *S. schimperi* growth characteristics and metabolites revealed positive correlations between growth parameters including leaves and root fresh and dry weights, chl *a*, chl *b*, total chlorophyll, betalains, GSH, palmitoleic, and linoleic acids (Figure 11). However, they were negatively associated with MDA, sucrose, soluble sugars, proline, starch, Na^+, Na^+/K^+ ratio, palmitic, and stearic acids. In addition, antioxidant enzymes including CAT, PPO, and APX were positively correlated with Na^+ and Na^+/K^+ ratio, GB, palmitoleic, linoleic, betanin, growth criteria, GSH, and chlorophylls.

DISCUSSION

The current study provides insights into the adaptive mechanisms of *S. schimperi* plants to cope with varying levels of salinity stress.

Changes in *S. schimperi* growth. Our growth analysis revealed that *S. schimperi* shows optimal growth at 200 mmol with lower and higher concentrations leading to significant growth impairment (Figure 1). These growth responses suggest that 200 mmol NaCl consistently promotes beneficial stress responses, enhancing *S. schimperi* performance across all metrics and time points, and confirming its obligate halophytic nature. This finding aligns with the reported moderate salinity-improved vegetative growth in other *Suaeda* spp. including *S. salsa*, *S. fruticose*, and *S. maritima* (Guo et al. 2019, Li et al. 2022) and other halophytes (Podar et al. 2019, Sogoni et al. 2021). These results coincide with the typical "curvilinear" growth response to salinity stress in halophytes, where peak growth occurs at intermediate salinity stress (Wang et al. 2023). The differential salinity-induced growth responses were more pronounced at 15 DAT rather than at 5 DAT, likely due to prolonged salt stress effects on root water and nutrient uptake, leading to cellular damage to *S. schimperi* plants (Tian et al. 2020), reduced turgor, and high energy demand for salt secretion and osmo-regulation (Mohammadi and Kardan 2016).

https://doi.org/10.17221/73/2025-PSE

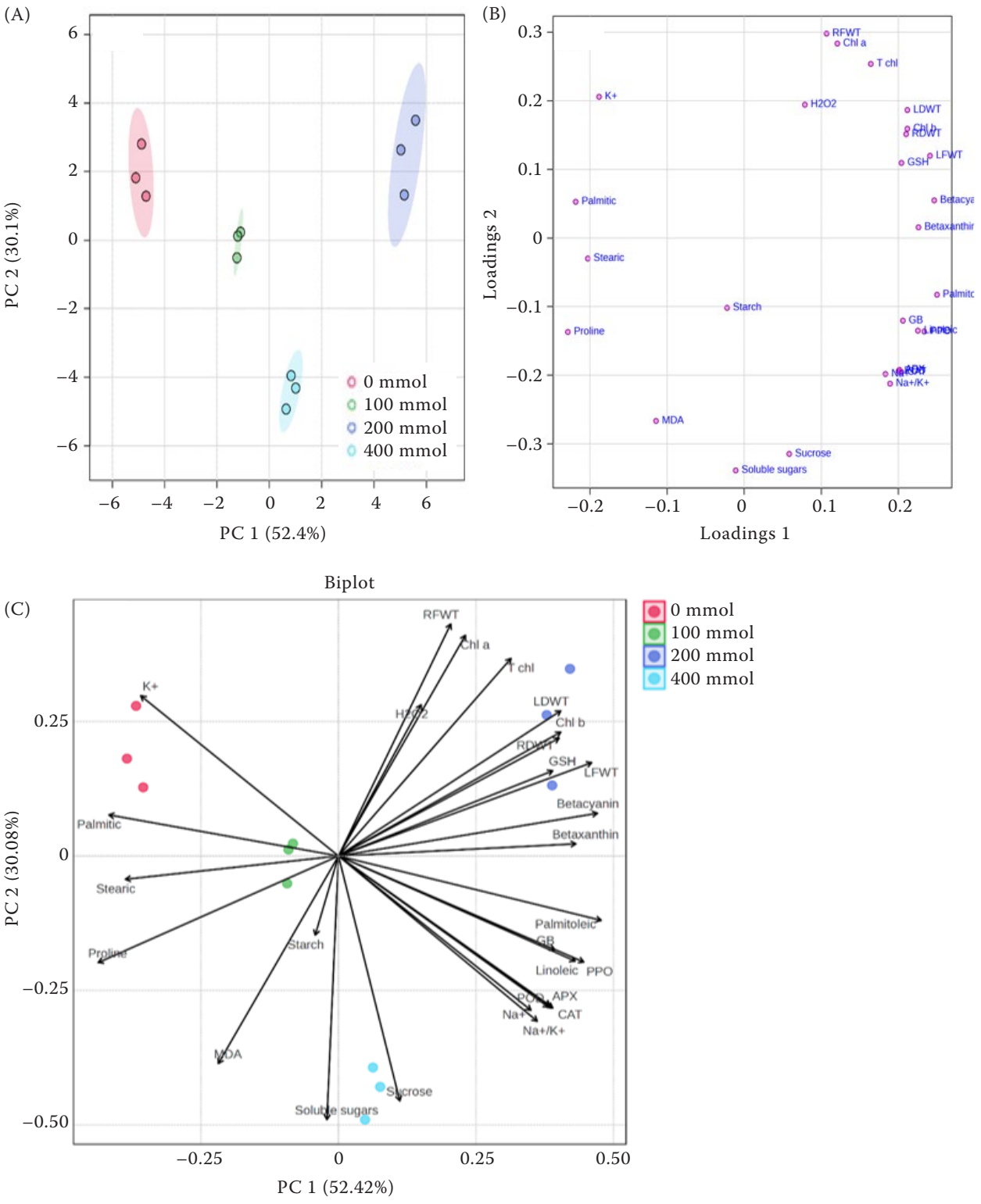

Figure 10. Principal component analysis (PCA) showing different responses of metabolites to varying salt stress conditions in the leaf of *Suaeda schimperi* across 2 sampling points 5 and 15 DAT. (A) PCA score plot; (B) PCA loading plot, and (C) PCA-biplot matrix. CAT – catalase activity; APX – ascorbate peroxidase; POD – peroxidase; PPO – polyphenol oxidase; GB – glycine betaine; GSH – glutathione; MDA – malonaldehyde; T chl – total chlorophyll; Chl *a* – chlorophyll *a*; Chl *b* – chlorophyll *b*; LFWT – leaves fresh weight; LDWT – leaves dry weight; RFWT – root fresh weight; RDWT – root dry weight

https://doi.org/10.17221/73/2025-PSE

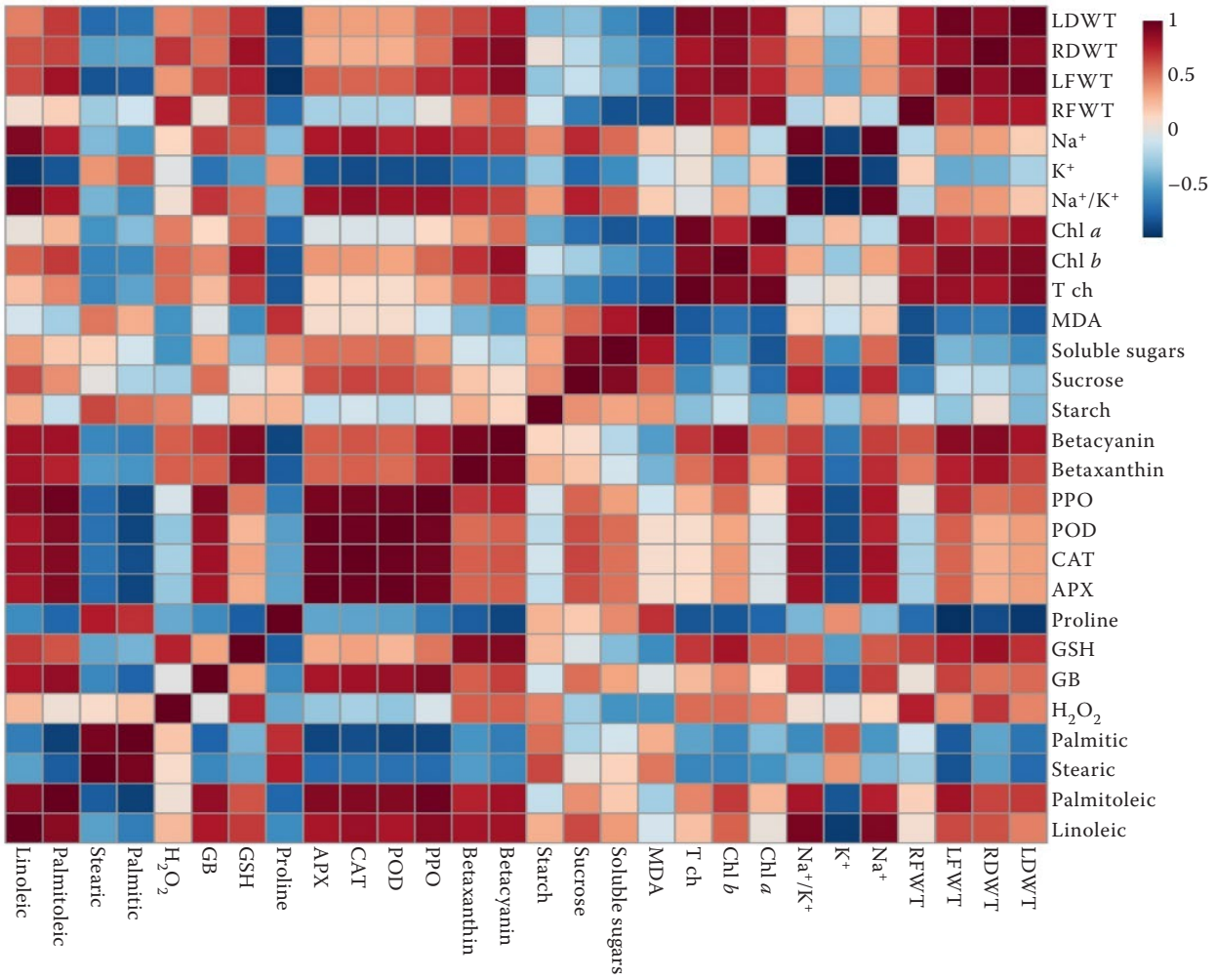

Figure 11. Correlation matrix between physiological and metabolic traits of *Suaeda schimperi* plants in response to varying salinity across 2 sampling points 5 and 15 DAT. The matrix was created using Pearson's coefficient of both control and NaCl-treated samples. Brown colour represents a positive correlation, and blue colour represents a negative correlation. CAT – catalase activity; APX – ascorbate peroxidase; POD – peroxidase; PPO – polyphenol oxidase; GB – glycine betaine; GSH – glutathione; MDA – malonaldehyde; T chl – total chlorophyll; Chl a – chlorophyll *a*; Chl b – chlorophyll *b*; LFWT – leaves fresh weight; LDWT – leaves dry weight; RFWT – root fresh weight; RDWT – root dry weight

Ionic balance. Our ionic analysis revealed a significant increase in Na^+ and a concurrent decrease in K^+ in leaves across all salt treatments (Figure 2). This differential ionic response is due to the competition between Na^+ and K^+ uptake, consistent with previous research (Zhang et al. 2021). Na^+ accumulation in halophytes is an adaptive response to salinity stress as they sequester excessive cytosolic Na^+ into the central vacuole to prevent cytoplasmic ionic toxicity, maintain ion homeostasis, increase osmotic potential; enhancing water uptake (Yamaguchi et al. 2013). The reduction in K^+ aligns with the responses of other succulent halophytes (Behr et al. 2017). The differential uptake of Na^+ and K^+ leads to an altered Na^+/K^+ ratio, particularly at 400 mmol NaCl (Figure 2), indicating ionic imbalance and explaining the adverse effect of high salinity on *S. schimperi* growth (Figure 1). Similar patterns were observed in *S. salsa* (Guo et al. 2019), *Tamarix chinensis* (Hussain et al. 2021), and other halophytes (Kumar et al. 2021). Maintaining an optimal Na^+/K^+ ratio is crucial for buffering physiological processes like photosynthesis and enzyme activity (Shabala and Mackay 2011).

Photosynthetic pigments dynamics. *S. schimperi* plants exposed to moderate salt concentration had the highest levels of chl *a*, chl *b*, and total chlorophyll across treatments at both time points, although levels were lower at 15 DAT (Figure 3). Similar responses

https://doi.org/10.17221/73/2025-PSE

have been observed in *S. salsa* (Li et al. 2023), and other plants like *Amaranthus tricolor* and *Tetragonia decumbens* (Wang and Nii 2000, Sogoni et al. 2021). These findings suggest healthy growth and enhanced photosynthetic activity of *S. schimperi* plants under moderate salinity, contributing to their improved biomass accumulation (Li et al. 2022). In contrast, the lower chlorophyll content in *S. schimperi* plants under low and high salt treatments indicates reduced chlorophyll synthesis and/or degradation, possibly due to salinity-induced damage to the thylakoid structure (Li et al. 2023) and inhibition of chlorophyll synthesis-related enzymes such as ALA-hydrogenase (Mohammadi and Kardan 2016), leading to impaired photosynthesis and retarded growth in *S. schimperi* plants under these conditions (Al-Shamsi et al. 2020).

Alteration in carbohydrate metabolism. *S. schimperi* plants exhibited differential responses in carbohydrate fractions across salinity levels, suggesting active carbon allocation as an adaptive strategy to saline conditions, consistent with previous reports (Gil et al. 2013, Zhao et al. 2017). Under low and medium stress, *S. schimperi* plants reduced their sucrose, TSS, and starch at 5 DAT, and such patterns were reversed at 15 DAT (Figure 4), reflecting a shift in growth and adaptation needs. Such temporal shift in carbohydrate response – initial reduction at 5 DAT followed by accumulation at 15 DAT (Figure 4) suggests a unique carbon allocation prioritisation strategy, where short-term carbon is diverted for immediate energy and growth needs, while accumulation under long-term exposure to salinity contributes to maintaining osmotic balance. Such a response has not been commonly documented in *Suaeda* species. Under high stress, an initial accumulation of sugars and starch at 5 DAT, followed by a decline at 15 DAT, suggests a potential osmoprotective role early on, which lessens by 15 DAT. A similar early induction of total soluble carbohydrates was observed in *Cakile maritima* plants under 400 mmol NaCl (Megdiche et al. 2007). Overall, the active changes in sucrose, TSS, and starch in the current study reflect their intricate involvement in the adaptive, remarkable resilience strategies in *S. schimperi* against salt stress. It is worth mentioning that soluble carbohydrates, even in low concentrations, have a pivotal role in salt tolerance, potentially through their ability to serve as chaperones or scavenge ROS through their antioxidative properties (Gil et al. 2013). Also, they act as osmolytes, regulating cells' turgor pressure and water uptake in saline soils. Further, soluble sugars protect proteins and cell membranes against salt stress-induced damage. Such responses help cells counteract salinity-oxidative damage and modulate the activity of various enzymes contributing to the regulation of ion transport processes essential for maintaining ionic balance and overall cellular ion homeostasis within plant cells. Besides that, soluble sugars are involved in signaling pathways regulating the expression of salt-responsive genes (Wungrampha et al. 2020).

Oxidative stress. *S. schimperi* plants displayed distinct patterns of oxidative stress markers, MDA and H_2O_2, across salinity levels. Moderate salinity-stressed plants had the lowest MDA concentration with 29% lower than non-saline conditions, particularly at 15 DAT (Figure 5), suggesting effective redox homeostasis due to efficient ROS detoxification through antioxidants. Similar responses were observed in *Crithmum maritimum* (Ben Amor et al. 2005) and *S. fruticose* (Gul et al. 2024). Elevated MDA under low- and high salinity reflects stronger oxidative stress and suggests potent salinity-induced lipid peroxidation, compromising membrane integrity, and partially explaining the retarded growth of *S. schimperi* plants under these salinity levels (Boughalleb et al. 2020). Regardless of the treatments, the *S. schimperi* plants had higher H_2O_2 levels at 15 DAT compared to 5 DAT. Unlike *S. fruiticosa* and *S. australis* where both MDA and H_2O_2 simultaneously increased as salinity stress increased (Hameed et al. 2012, Qu et al. 2024), *S. schimperi* exhibits decoupled dynamics between H_2O_2 and MDA under the tested levels of salinity stress (Figure 5). This finding indicates that *S. schimperi* plants possess robust H_2O_2-scavenging systems (CAT, POD; see below) that mitigate H_2O_2 without preventing lipid peroxidation from other ROS types. Such selective ROS detoxification is relatively unexplored and adds novelty to the redox regulatory strategies of *S. schimperi*.

Osmolytes and antioxidant metabolites. *S. schimperi* plants under moderate salinity stress consistently had the lowest proline content, while those under high salt showed significantly higher proline, particularly at 5 DAT, suggesting an early proline response to high salinity stress (Figure 6). This aligns with the stimulative effects of high salinity on proline synthesis (Huang et al. 2013). However, the link between proline and salinity adaptation is not always observed (Bueno et al. 2020). In contrast, *S. schimperi* plants under moderate and high salinity showed increased GB compared to the non-saline

https://doi.org/10.17221/73/2025-PSE

conditions only at 15 DAT (Figure 6), suggesting its role in long-term osmotic adjustment (Flowers and Colmer 2015, Patel et al. 2016). The moderate and high salt-induced GB accumulation has also been observed in *S. aralocaspica* and *B. sinuspersici* (Park et al. 2009). GB contributes to the maintenance of photosynthetic activity *via* adjustment of stromal enzymes and protection of thylakoid membranes (Ayub et al. 2022) and protecting the photosystem II (PS-II) complex under salinity (Murata et al. 1992).

Interestingly, *S. schimperi* leaves showed coordinated higher accumulation of GSH, betacyanin, and betaxanthin with increasing salinity, peaking under moderate stress (Figure 7). This aligns with the reported salinity-induced synthesis of betacyanin and GSH in *S. salsa* (Wang et al. 2007, Li et al. 2020) and *S. schimperi* plants grown under high salinity in their natural hyper-arid salt marches (Ibraheem et al. 2022). These findings support the potential role of these secondary metabolites in salt tolerance in *S. schimperi via* quenching ROS and maintaining redox homeostasis, and osmotic balance by regulating cell osmotic pressure (Gliszczyńska-Świgło et al. 2006) as well as photoprotection of chloroplasts (Jain and Gould 2015). These responses partially explain the higher chlorophyll levels and lower MDA in *S. schimperi* plants under moderate salinity (Figures 3 and 5). Interestingly, unlike in *S. japonica* and *S. salsa*, where an inverse relationship between chlorophyll and betacyanin accumulation was observed during growth (Hayakawa and Agarie 2010, Cai et al. 2025), *S. schimperi* plants maintained a relatively similar response in both chlorophyll and betacyanin levels under salinity stress. This response suggests a special capability of *S. schimperi* to simultaneously enhance its primary photosynthetic capacity and antioxidant defenses under saline conditions. The simultaneous enhancement in these two critical traits partially explains the observed sugar accumulation under salinity at 15 DAT.

Along with the above non-enzymic metabolite responses, *S. schimperi* plants increased their foliar activity of PPO, POD, CAT, and APX in response to salinity, peaking under medium salinity at 5 DAT (Figure 8). At 15 DAT, the highest enzyme activities were observed under high salinity, whereas low and moderate salinity levels resulted in similar (PPO and POD), or lower (APX) activities compared to the non-saline conditions. CAT activity under low salinity was similar to the non-saline condition, but significantly higher under moderate salinity. These changes reflect the crucial role of antioxidant enzymes in detoxifying salinity-induced ROS (Pirasteh-Anosheh et al. 2023). Peaking enzyme activities under 200 mmol at 5 DAT suggest an optimal balance between ROS production and scavenging, supporting better growth under moderate salinity. Similar roles of CAT and APX have been observed in salinity-stressed *S. salsa* and *S. maritima* (Wu et al. 2012, Li et al. 2020). In contrast, the decline in the activities of the tested enzymes at 400 mmol NaCl at 5 DAT suggests that the overall plant antioxidant capacity may become overwhelmed, leading to oxidative damage and growth suppression, consistent with the finding that salinity over 300 mmol induces ROS accumulation and stunts growth (Ben Hamed et al. 2007, Souid et al. 2016).

S. schimperi plants decreased their palmitic and stearic acids content as salinity rose, while palmitoleic and linoleic acids peaked at 200 mmol NaCl and slightly decreased at 400 mmol NaCl (Figure 9). This coincides with the accumulation of unsaturated fatty acids in salinity-stressed *S. salsa* (Li and Song 2019) and the reduction of saturated fatty acids in the xero-halophyte *Haloxylon salicornicum* under salinity (Panda et al. 2021). The increase in palmitoleic and α-linoleic acids aligns with the role of the unsaturated fatty acids in maintaining membrane fluidity and cellular homeostasis under stress (Li and Song 2019). These fatty acids also benefit jasmonic acid biosynthesis, activating antioxidant pathways, suggesting that *S. schimperi* plants may invest in their biosynthesis and use them as adaptive mechanisms against the severe salt stress they encounter (López-Pérez et al. 2009). The salinity-induced reduction in saturated acids like stearic and palmitic acids may result from increased β-oxidation, providing the energy necessary to help plants cope with salt stress (Panda et al. 2021).

The ability of *S. schimperi* to upregulate key antioxidants and osmo-protectants highlights its potential as a valuable genetic reservoir for stress resilience traits in halophytes and crops, particularly, those grown in marginal or moderately saline soils. The special capability of *S. schimperi* to simultaneously enhance its primary photosynthetic capacity and antioxidant defenses under saline conditions holds promise for biotechnological exploitation in agriculture in salt-affected lands. Future characterisation of *S. schimperi*'s responses at the molecular level will be crucial for uncovering candidate genes for developing salt-tolerant crops.

Acknowledgement. The authors extend their appreciation to Umm Al-Qura University, Saudi Arabia for funding this research work through grant number: 25UQU4350597GSSR01.

https://doi.org/10.17221/73/2025-PSE

REFERENCES

Agarwal S., Shaheen R. (2007): Stimulation of antioxidant system and lipid peroxidation by abiotic stresses in leaves of *Momordica charantia*. Brazilian Journal of Plant Physiology, 19: 149–161.

Ahmed M., Tóth Z., Decsi K. (2024): The impact of salinity on crop yields and the confrontational behaviour of transcriptional regulators, nanoparticles, and antioxidant defensive mechanisms under stressful conditions: a review. International Journal of Molecular Sciences, 25: 2654.

Alexieva V., Sergiev I., Mapelli S., Karanov E. (2001): The effect of drought and ultraviolet radiation on growth and stress markers in pea and wheat. Plant, Cell and Environment, 24: 1337–1344.

Al-Shamsi N., Hussain M.I., El-Keblawy A. (2020): Physiological responses of the xerohalophyte *Suaeda vermiculata* to salinity in its hyper-arid environment. Flora, 273: 151705.

Ayub M.A., Rehman M.Z.U., Umar W., Farooqi Z.U.R., Sarfraz M., Ahmad H.R., Ahmad Z., Aslam M.Z. (2022): Role of glycine betaine in stress management in plants. Emerging Plant Growth Regulators in Agriculture: Roles in Stress Tolerance, 2022: 335–356.

Bates L.S., Waldren R.P., Teare I.D. (1973): Rapid determination of free proline for water-stress studies. Plant and Soil, 39: 205–207.

Behr J.H., Bouchereau A., Berardocco S., Seal C.E., Flowers T.J., Zörb C. (2017): Metabolic and physiological adjustment of *Suaeda maritima* to combined salinity and hypoxia. Annals of Botany, 119: 965–976.

Ben Amor N., Ben Hamed K., Debez A., Grignon C., Abdelly C. (2005): Physiological and antioxidant responses of the perennial halophyte *Crithmum maritimum* to salinity. Plant Science, 168: 889–899.

Ben Hamed K., Castagna A., Salem E., Ranieri A., Abdelly C. (2007): Sea fennel (*Crithmum maritimum* L.) under salinity conditions: a comparison of leaf and root antioxidant responses. Plant Growth Regulation, 53: 185–194.

Boughalleb F., Abdellaoui R., Mahmoudi M., Bakhshandeh E. (2020): Changes in phenolic profile, soluble sugar, proline, and antioxidant enzyme activities of *Polygonum equisetiforme* in response to salinity. Turkish Journal of Botany, 44: 25–35.

Boulos L. (1999): Flora of Egypt. Cairo, Al Hadara Publishing, 419.

Bueno M., Lendínez M.L., Calero J., del Pilar Cordovilla M. (2020): Salinity responses of three halophytes from inland saltmarshes of Jaén (southern Spain). Flora, 266: 151589.

Cai L.Y., Li M., Shen Y.F., Jiang R.T., Wang J.W., Ma S.Z., Wu M.Q., He P.M. (2025): Betacyanin accumulation mediates photosynthetic protection in *Suaeda salsa* (L.) Pall. under salt stress. Planta, 261: 100.

Castillo J.M., Mancilla-Leytón J.M., Martins-Noguerol R., Moreira X., Moreno-Pérez A.J., Muñoz-Vallés S., Pedroche J.J., Figueroa M.E., García-González A., Salas J.J., Cambrollé J. (2022): Interactive effects between salinity and nutrient deficiency on biomass production and bio-active compounds accumulation in the halophyte *Crithmum maritimum*. Scientia Horticulturae, 301: 111136.

Collenette S. (1985): Illustrated Guide to the Flowers of Saudi Arabia. London, Scorpion.

Darbyshire I., Pickering H., Kordofani M., Farag I., Candiga R. (2015): The plants of Sudan and South Sudan: An Annotated Checklist. Kew, Royal Botanic Gardens, 400.

Devi P. (2002): Principles and Methods in Plant Molecular, Biology, Biochemistry and Genetics. Jodhpur, Agrobios. ISBN-10: 8188826286

Diao F., Dang Z., Xu J., Ding S., Hao B., Zhang Z., Zhang J., Wang L., Guo W. (2021): Effect of arbuscular mycorrhizal symbiosis on ion homeostasis and salt tolerance-related gene expression in halophyte *Suaeda salsa* under salt treatments. Microbiological Research, 245: 126688.

Edwards S., Tadesse M., Demissew S., Hedberg I. (2000): Flora of Ethiopia and Eritrea, 2, The National Herbarium, Addis Ababa University, Department of Systematic Botany, Upps, 532.

Flowers T.J., Colmer T.D. (2015): Plant salt tolerance: adaptations in halophytes. Annals of Botany, 115: 327–331.

Gil R., Boscaiu M., Lull C., Bautista I., Lidón A., Vicente O. (2013): Are soluble carbohydrates ecologically relevant for salt tolerance in halophytes? Functional Plant Biology, 40: 805–818.

Gliszczyńska-Świgło A., Szymusiak H., Malinowska P. (2006): Betanin, the main pigment of red beet: molecular origin of its exceptionally high free radical-scavenging activity. Food Additives and Contaminants, 23: 1079–1087.

Grieve C.M., Grattan S.R. (1983): Rapid assay for determination of water soluble quaternary ammonium compounds. Plant and Soil, 70: 303–307.

Gul B., Hameed A., Ahmed M., Hussain T., Rasool S., Nielsen B. (2024): Thriving under salinity: growth, ecophysiology and proteomic insights into the tolerance mechanisms of obligate halophyte *Suaeda fruticosa*. Plants, 13: 1529.

Guo J., Dong X., Han G., Wang B. (2019): Salt-enhanced reproductive development of *Suaeda salsa* L. coincided with ion transporter gene upregulation in flowers and increased pollen K^+ content. Frontiers in Plant Science, 10: 1–17.

Guo J., Du M., Lu C., Wang B. (2020): NaCl improves reproduction by enhancing starch accumulation in the ovules of the euhalophyte *Suaeda salsa*. BMC Plant Biology, 20: 1–16.

Hameed A., Hussain T., Gulzar S., Aziz I., Gul B., Khan M.A. (2012): Salt tolerance of a cash crop halophyte *Suaeda fruticosa*: biochemical responses to salt and exogenous chemical treatments. Acta Physiologiae Plantarum, 34: 2331–2340.

Hansen J., Møller I. (1975): Percolation of starch and soluble carbohydrates from plant tissue for quantitative determination with anthrone. Analytical Biochemistry, 68: 87–94.

Hayakawa K., Agarie S. (2010): Physiological roles of betacyanin in a halophyte, *Suaeda japonica* Makino. Plant Production Science, 13: 351–359.

Huang Z., Zhao L., Chen D., Liang M., Liu Z., Shao H., Long X. (2013): Salt stress encourages proline accumulation by regulat-

https://doi.org/10.17221/73/2025-PSE

ing proline biosynthesis and degradation in Jerusalem artichoke plantlets. Plos One, 8: e62085.

Hussain T., Khan M. (2022): Empirical values of halophytes in agro-ecology and sustainability. Earth Systems Protection and Sustainability, 1: 57–78.

Hussain T., Li J., Feng X., Asrar H., Gul B., Liu X. (2021): Salinity induced alterations in photosynthetic and oxidative regulation are ameliorated as a function of salt secretion. Journal of Plant Research, 134: 779–796.

Ibraheem F., Al-Zahrani A., Mosa A. (2022): Physiological adaptation of three wild halophytic *Suaeda* species: salt tolerance strategies and metal accumulation capacity. Plants, 11: 537.

Jain G., Gould K.S. (2015): Functional significance of betalain biosynthesis in leaves of *Disphyma australe* under salinity stress. Environmental and Experimental Botany, 109: 131–140.

Joshi A., Rajput V.D., Verma K.K., Minkina T., Ghazaryan K., Arora J. (2023): Potential of *Suaeda nudiflora* and *Suaeda fruticosa* to adapt to high salinity conditions. Horticulturae, 9: 1–18.

Kumar A., Mann A., Kumar A., Kumar N., Meena B.L. (2021): Physiological response of diverse halophytes to high salinity through ionic accumulation and ROS scavenging. International Journal of Phytoremediation, 23: 1041–1051.

Li H., Wang H., Wen W., Yang G. (2020): The antioxidant system in *Suaeda salsa* under salt stress. Plant Signaling and Behavior, 15: 1771939.

Li J., Wang Y., Bao J., Ding Z., Yisilam G., Chu Z., Su Y., Wang Q., Tian X. (2023): Morphological and physiological responses of *Suaeda salsa* under drought and salt stress. Research Square. doi.org/10.21203/rs.3.rs-3255941/v1

Li Q., Liu R., Li Z., Fan H., Song J. (2022): Positive effects of NaCl on the photoreaction and carbon assimilation efficiency in *Suaeda salsa*. Plant Physiology and Biochemistry, 177: 32–37.

Li Q., Song J. (2019): Analysis of widely targeted metabolites of the euhalophyte *Suaeda salsa* under saline conditions provides new insights into salt tolerance and nutritional value in halophytic species. BMC Plant Biology, 19: 1–11.

Lichtenthaler H.K., Wellburn A.R. (1983): Determinations of total carotenoids and chlorophylls *a* and *b* of leaf extracts in different solvents. Biochemical Society Transactions, 11: 591–592.

López-Pérez L., Martínez-Ballesta M. del C., Maurel C., Carvajal M. (2009): Changes in plasma membrane lipids, aquaporins and proton pump of broccoli roots, as an adaptation mechanism to salinity. Phytochemistry, 70: 492–500.

Megdiche W., Amor N. Ben, Debez A., Hessini K., Ksouri R., Zuily-Fodil Y., Abdelly C. (2007): Salt tolerance of the annual halophyte *Cakile maritima* as affected by the provenance and the developmental stage. Acta Physiologiae Plantarum, 29: 375–384.

Mohammadi H., Kardan J. (2016): Morphological and physiological responses of some halophytes to salinity stress. Annales Universitatis Mariae Curie-Sklodowska, Sectio C – Biologia, 70: 31.

Mujeeb A., Aziz I., Ahmed M.Z., Shafiq S., Fatima S., Alvi S.K. (2021): Spatial and seasonal metal variation, bioaccumulation and biomonitoring potential of halophytes from littoral zones of the Karachi Coast. Science of The Total Environment, 781: 146715.

Murata N., Mohanty P.S., Hayashi H., Papageorgiou G.C. (1992): Glycine betaine stabilizes the association of extrinsic proteins with the photosynthetic oxygen-evolving complex. FEBS Letters, 296: 187–189.

Ouyang S.Q., Liu Y.F., Liu P., Lei G., He S.J., Ma B., Zhang W.K., Zhang J.S., Chen S.Y. (2010): Receptor-like kinase OsSIK1 improves drought and salt stress tolerance in rice (*Oryza sativa*): plants. The Plant Journal, 62: 316–329.

Panda A., Rangani J., Parida A.K. (2021): Unravelling salt responsive metabolites and metabolic pathways using non-targeted metabolomics approach and elucidation of salt tolerance mechanisms in the xero-halophyte *Haloxylon salicornicum*. Plant Physiology and Biochemistry, 158: 284–296.

Park J., Okita T.W., Edwards G.E. (2009): Salt tolerant mechanisms in single-cell C4 species *Bienertia sinuspersici* and *Suaeda aralocaspica* Chenopodiaceae. Plant Science, 176: 616–626.

Patel M.K., Mishra A., Jha B. (2016): Untargeted metabolomics of halophytes. In: Kim S.-K. (ed.): Marine Omics. Boca Raton, CRC Press, 307–325. ISBN: 9781315372303

Pirasteh-Anosheh H., Samadi M., Kazemeini S.A., Ozturk M., Ludwiczak A., Piernik A. (2023): ROS homeostasis and antioxidants in the halophytic plants and seeds. Plants, 12: 3023.

Podar D., Macalik K., Réti K.O., Martonos I., Török E., Carpa R., Weindorf D.C., Csiszár J., Székely G. (2019): Morphological, physiological and biochemical aspects of salt tolerance of halophyte *Petrosimonia triandra* grown in natural habitat. Physiology and Molecular Biology of Plants, 25: 1335–1347.

Pungin A., Lartseva L., Loskutnikova V., Shakhov V., Popova E., Skrypnik L., Krol O. (2023): Effect of salinity stress on phenolic compounds and antioxidant activity in halophytes *Spergularia marina* (L.): Griseb. and *Glaux maritima* L. cultured *in vitro*. Plants, 12: 1905.

Qu Y., Wang J., Qu C., Mo X., Zhang X. (2024): Genome-wide identification of WRKY in *Suaeda australis* against salt stress. Forests, 15: 1297.

Raymond J., Rakariyatham N., Azanza J. (1993): Purification and some properties of polyphenoloxidase from sunflower seeds. Phytochemistry, 34: 927–931.

Sadasivam S. (1996): Biochemical Methods. New Delhi, New Age International Publishers.

Shabala S., Mackay A. (2011): Ion transport in halophytes. Advances in Botanical Research, 57: 151–199.

Sinha A.K. (1972): Colorimetric assay of catalase. Analytical Biochemistry, 47: 389–394.

Skalicky M., Kubes J., Shokoofeh H., Tahjib-Ul-Arif M., Vachova P., Hejnak V. (2020): Betacyanins and betaxanthins in cultivated varieties of *Beta vulgaris* L. compared to weed beets. Molecules, 25: 1–15.

Sogoni A., Jimoh M.O., Kambizi L., Laubscher C.P. (2021): The impact of salt stress on plant growth, mineral composition, and

https://doi.org/10.17221/73/2025-PSE

antioxidant activity in *Tetragonia decumbens* Mill.: an underutilized edible halophyte in South Africa. Horticulturae, 7: 140.

Souid A., Gabriele M., Longo V., Pucci L., Bellani L., Smaoui A., Abdelly C., Ben Hamed K. (2016): Salt tolerance of the halophyte *Limonium delicatulum* is more associated with antioxidant enzyme activities than phenolic compounds. Functional Plant Biology, 43: 607–619.

Thulin M., Beier B.A., Razafimandimbison S.G., Banks H.I. (2008): Ambilobea, a new genus from Madagascar, the position of aucoumea, and comments on the tribal classification of the frankincense and myrrh family (Burseraceae). Nordic Journal of Botany, 26: 218–229.

Tian F., Hou M., Qiu Y., Zhang T., Yuan Y. (2020): Salinity stress effects on transpiration and plant growth under different salinity soil levels based on thermal infrared remote (TIR): technique. Geoderma, 357: 113961.

Wang C.Q., Chen M., Wang B.S. (2007): Betacyanin accumulation in the leaves of C3 halophyte *Suaeda salsa* L. is induced by watering roots with H_2O_2. Plant Science, 172: 1–7.

Wang N., Zhao Z., Zhang X., Liu S., Zhang K., Hu M. (2023): Plant growth, salt removal capacity, and forage nutritive value of the annual euhalophyte *Suaeda salsa* irrigated with saline water. Frontiers in Plant Science, 13: 1–13.

Wang Y., Nii N. (2000): Changes in chlorophyll, ribulose bisphosphate carboxylase-oxygenase, glycine betaine content, photosynthesis and transpiration in *Amaranthus tricolor* leaves during salt stress. The Journal of Horticultural Science and Biotechnology, 75: 623–627.

Wu H.F., Liu X.L., You L.P., Zhang L.B., Zhou D., Feng J.H., Zhao J., Yu J.B. (2012): Effects of salinity on metabolic profiles, gene expressions, and antioxidant enzymes in halophyte *Suaeda salsa*. Journal of Plant Growth Regulation, 31: 332–341.

Wungrampha S., Rawat N., Lata Singla-Pareek S., Pareek A. (2020): Survival strategies in halophytes: adaptation and regulation. In: Grigore M.-N. (ed.): Handbook of Halophytes. From Molecules to Ecosystems towards Biosaline Agriculture. Cham, Springer International Publishing, 1–22.

Yamaguchi T., Hamamoto S., Uozumi N. (2013): Sodium transport system in plant cells. Frontiers in Plant Science, 4: 65912.

Zahran H.A., Tawfeuk H.Z. (2019): Physicochemical properties of new peanut (*Arachis hypogaea* L.) varieties. OCL, 26: 19.

Zang W., Miao R., Zhang Y., Yuan Y., Pang Q., Zhou Z. (2021): Metabolic and molecular basis for the salt and alkali responses of *Suaeda corniculata*. Environmental and Experimental Botany, 192: 104643.

Zhang J.L., Bai R., Flowers T.J., Wang C.M., Wetson A.M., Duan H.R., He A.L., Gurmani A.R., Wang S.M. (2021): Dynamic responses of the halophyte *Suaeda maritima* to various levels of external NaCl concentration. In: Grigore M.-N. (ed.): Handbook of Halophytes. From Molecules to Ecosystems towards Biosaline Agriculture. Cham, Springer International Publishing, 1637–1657.

Zhao L., Yang Z., Guo Q., Mao S., Li S., Sun F., Wang H., Yang C. (2017): Transcriptomic profiling and physiological responses of halophyte *Kochia sieversiana* provide insights into salt tolerance. Frontiers in Plant Science, 8: 1–13.

Received on: February 23, 2025
Accepted on: May 5, 2025
Published online: May 23, 2025